Rubin, J. R., & Sundaralingam, M. (1983) *J. Biomol. Struct. Dyn. 1*, 639–646.
Rubin, J. R., Wang, J., & Sundaralingam, M. (1983) *Biochim. Biophys. Acta 756*, 111–118.
Ruffner, D. E., & Uhlenbeck, O. C. (1990) *Nucleic Acids Res. 18*, 6025–6029.
Ruffner, D. E., Dahm, S. C., & Uhlenbeck, O. C. (1989) *Gene 82*, 31–41.
Shapiro, R., & Vallee, B. L. (1989) *Biochemistry 28*, 7401–7408.
Steffens, J. J., Siewers, I. J., & Benkovic, S. J. (1975) *Biochemistry 14*, 2431–2440.
Stein, A., & Crothers, D. M. (1976) *Biochemistry 15*, 157–160.
Teeter, M., Quigley, G., & Rich, A. (1981) in *Metal Ions in Genetic Information Transfer* (Eichhorn, G. L., & Marzilli, L. G., Eds.) pp 233–272, Elsevier North-Holland, Inc., New York.
Uhlenbeck, O. C. (1987) *Nature 328*, 596–600.
Weast, R. C. (1987) *Handbook of Chemistry and Physics*, 68th ed., CRC Press, Boca Raton, FL.
Werner, C., Krebs, B., Keith, G., & Dirheimer, G. (1976) *Biochim. Biophys. Acta 432*, 161–175.

# Actinomycin D and 7-Aminoactinomycin D Binding to Single-Stranded DNA

Randy M. Wadkins‡ and Thomas M. Jovin*
*Department of Molecular Biology, Max Planck Institute for Biophysical Chemistry, Postfach 2841, W-3400 Göttingen, Federal Republic of Germany*
*Received March 6, 1991; Revised Manuscript Received July 3, 1991*

ABSTRACT: The potent RNA polymerase inhibitors actinomycin D and 7-aminoactinomycin D are shown to bind to single-stranded DNAs. The binding occurs with particular DNA sequences containing guanine residues and is characterized by hypochromic UV absorption changes similar to those observed in interactions of the drugs with double-stranded duplex DNAs. The most striking feature of the binding is the dramatic (ca. 37-fold) enhancement in fluorescence that occurs when the 7-aminoactinomycin is bound to certain single-stranded DNAs. This fluorescence of the complex is also characterized by a 40-nm hypsochromic shift in the emission spectrum of the drug and an increase in the emission anisotropy relative to the free drug or the drug bound to calf thymus DNA. The fluorescence lifetimes change in the presence of the single-stranded DNA in a manner compatible with the intensity difference. Thus, there is an increase in the fraction of the emission corresponding to a 2-ns lifetime component compared to the predominant ~0.5-ns lifetime of the free drug. The 7-aminoactinomycin D comigrates in polyacrylamide gels with the single-stranded DNAs, and the fluorescence of the bound drug can be visualized by excitation with 540-nm light. The binding interactions are characterized by association constants of $2.0 \times 10^6$ to $1.1 \times 10^7$ $M^{-1}$.

Actinomycin D (ACTD)[1] is a compound with a variety of biological properties [for a review, see Waring, (1981)]. It has been used clinically to treat numerous tumors (Farber, 1966; Lewis, 1972). It is also a potent inhibitor of transcription both in vivo (Goldberg & Friedman, 1971; Kersten & Kersten, 1974) and in vitro (Reich, 1964; Wells & Larson, 1970; Straney & Crothers, 1987; White & Phillips, 1988). The transcriptional inhibition is thought to occur through binding of the drug to DNA and blockage of the RNA polymerase during elongation (Mueller & Crothers, 1968; Sentenac et al., 1968; Aivasashvilli & Beabealashvilli, 1983; Straney & Crothers, 1987; White & Phillips, 1988), inasmuch as ACTD has not been observed to bind to RNA (Goldberg & Friedman, 1971; Kersten & Kersten, 1974; Bunte et al., 1980).

The binding of ACTD to DNA is characterized by a general requirement for G/C residues that can be fullfilled by either a $^5$G–C$^3$ or $^5$C–G$^3$ step. However, the binding to the latter sequence is substantially weaker (Wilson et al., 1986; Chen, 1988; Zhou et al., 1989). Crystal structures of the drug complexed with dG and dGpdC suggest that the structural basis for the G/C requirement is the need for hydrogen bonding between the carboxyl of the threonine residue of the drug and the guanine exocyclic 2-amino protons (Jain & Sobell, 1972; Takusagawa et al., 1982). Additionally, the flanking base pairs at such G–C or C–G steps also greatly influence the binding properties of the drug (Chen, 1988a,b, 1990; White & Phillips, 1988), making it clear that the mechanism of binding of ACTD is complex and cannot be specified by a simple nearest-neighbor requirement.

ACTD also binds to sequences that do not contain either G–C or C–G sites, for example poly(dI) (Wells & Larson, 1970). In addition, binding of the drug has been observed to the synthetic polynucleotides poly[d(GTA)]·poly[d(TAC)], poly[d(GAA)]·poly[d(TTC)], and poly[d(TTG)]·poly[d(CAA)], all of which contain only a single d(G·C) base pair in tracts of A's and T's (Wells & Larson, 1970). Interestingly, no interaction was observed with poly[d(GAT)]·poly[d(ATC)], emphasizing that the sequence of the DNA is the primary

* To whom correspondence should be addressed.
‡ Present address: Department of Biochemical & Clinical Pharmacology, St. Jude Children's Research Hospital, Memphis, TN.

[1] Abbreviations: ACTD, actinomycin D; 7AACTD, 7-aminoactinomycin D; TBE, 90 mM tris(hydroxymethyl)aminomethane, 90 mM boric acid, 2.5 mM ethylenediaminetetraacetic acid, pH 8.3; TBM, 90 mM tris(hydroxymethyl)aminomethane, 90 mM boric acid, 2.5 mM $MgCl_2$, pH 8.3.

0006-2960/91/0430-9469$02.50/0 

```
D1:   5'-AAAAAAAAAATAATTTTAAATATTT-3'
D2:   5'-TTTTTTTTTTATTAAAATTTATAAA-3'
D5:   5'-AAAAAGAAAGTAGTTTTAAGTATTT-3'
D6:   5'-TTTTTCTTTCATCAAAATTCATAAA-3'
D7:   5'-AAATACTTAAAACTACTTTCTTTTT-3'
F9:   5'-TTTTTATGAAATATA-3'
PL7:  5'-CTCGACGG-3'
```

FIGURE 1: Sequences of oligonucleotides used in these studies. Strands designated D5 and D6 form parallel duplexes with bases in the reverse Watson–Crick motif (Rippe et al., 1990). Strands designated D5 and D7 form standard Watson–Crick base-paired double helices. Note that the trimeric sequence for the guanine residues are $^5$'AGA$^3$' and $^5$'AGT$^3$' for D5, $^5$'TGA$^3$' for F9, and $^5$'CGA$^3$' and $^5$'CGG$^3$' for PL7.

determinant of the ACTD–DNA interaction.

In this report, we have extended the studies of the interactions of ACTD with DNA to include complexes formed by the drug with defined single-stranded sequences. We have used primarily the fluorescent derivative of ACTD, 7-aminoactinomycin D (7AACTD), to characterize the binding. 7AACTD was first reported by Sengupta et al. (1975) and has been shown to mimic ACTD in its ability to bind double-stranded DNA (Gill et al., 1975; Chiao et al., 1979; Graves & Wadkins, 1989). Despite the vast literature concerning ACTD, the binding to single-stranded DNA has received scant attention and in general has been attributed to residual helical structure (Reich, 1964). This is surprising in light of the potent inhibition by ACTD of RNA polymerase and the obvious importance of interactions between polymerase and single-stranded DNA segments. We have found that 7AACTD binds better to certain single-stranded sequences than to double-stranded native and synthetic DNAs. The mechanism of this binding appears to involve stacked complexes between the drug and the single-stranded DNA. The binding to single-stranded DNA, as is the case with double-stranded DNA, is highly dependent on the sequence. The possible biological significance of this phenomenon is discussed.

## Materials and Methods

*Materials.* Actinomycin D and 7-aminoactinomycin D were purchased from Sigma and used without further purification. The synthetic DNAs designated D1, D5, D6, D7, F9, and PL7 [Figure 1; designations were chosen on the basis of previous work with synthetic fragments from this laboratory (Jovin et al., 1990)] were synthesized by use of standard solid-phase synthesis techniques on an Applied Biosystems (Foster City, CA) synthesizer as described elsewhere (Rippe et al., 1989). Poly(dG) and poly(dI) were purchased from Pharmacia.

The choice of DNA sequences resulted from investigations of ligand binding to parallel-stranded DNA (Rippe et al., 1990). It was found that 7AACTD binds to parallel-stranded DNA sequences containing d(G·C) base pairs (the D5·D6 parallel-stranded duplex); this work will be presented elsewhere (R. M. Wadkins and T. M. Jovin, manuscript in preparation). However, during the course of the control experiments, it became evident that 7AACTD also binds to the single-stranded oligonucleotide D5, leading to the experiments described here. The additional sequences F9 and PL7 contained guanine residues and were non-self-complementary, ensuring their single-stranded nature.

Concentrations of DNA were determined by use of the molar (base) absorptivities 8.6 $mM^{-1}$ $cm^{-1}$ for D1, D5, D7, and F9; 8.4 $mM^{-1}$ for D6; and 8.1 $mM^{-1}$ $cm^{-1}$ for PL7, at 264 nm and 70 °C (Jovin et al., 1990). Molar (nucleotide) absorptivities for other DNAs at 260 nm and 20 °C are 6.6 $mM^{-1}$ $cm^{-1}$ for calf thymus DNA, 9.0 $mM^{-1}$ $cm^{-1}$ for poly(dG), 5.35 $mM^{-1}$ $cm^{-1}$ for poly(dI) (Bollum, 1967), and 26.3 $mM^{-1}$ (dinucleotides) $cm^{-1}$ for dCpG. Concentrations of 7AACTD and ACTD were determined by use of the molar absorptivities 21.9 $mM^{-1}$ $cm^{-1}$ at 505 nm (Gill et al., 1975) and 24.4 $mM^{-1}$ $cm^{-1}$ at 440 nm (Bittman & Blau, 1975), respectively.

*Spectroscopic Experiments.* All experiments were performed in 2 mM $MgCl_2$/10 mM sodium cacodylate buffer adjusted to pH 7.1. The temperature was maintained with use of a regulating water bath. Corrected fluorescence excitation and emission spectra and fluorescence polarization spectra were obtained by use of an SLM (Urbana–Champaign, IL) 8000 photon-counting spectrofluorometer. Excitation wavelengths were chosen to maximize the signal from the bound species and are reported in Table I. Absorption spectra were recorded on an Uvikon 820 UV–visible spectrophotometer. Temperature-resolved UV–visible spectra were obtained with use of the spectrophotometer interfaced to a DEC Micro VAX minicomputer as described previously (Ramsing & Jovin, 1988; Ramsing et al., 1989). Acquisition was over a 3–86 °C temperature range, and the data were analyzed as described previously (Ramsing et al., 1989).

Titration curves were derived from the change in the fluorescence signal of 7AACTD upon addition of DNA. The inverse experiment, addition of drug to a DNA solution, was also performed for the D5–7AACTD interactions. The excitation wavelength was chosen to maximize the bound drug signal (Table I), and the emission was measured using an Orion band-pass filter centered at 630 nm with a 10-nm half-width.

Association constants for 7AACTD binding to DNA were obtained from the simple site interaction model

$$L + D \Leftrightarrow LD \tag{1}$$

which gives rise to

$$K_a = [LD]/([L][D]) \tag{1a}$$

in which [LD] and [L] are the concentrations of bound and free 7AACTD, respectively, and [D] is the concentration of DNA in sites. We assumed a model incorporating $n$ equivalent, noninteracting sites per DNA strand. Thus

$$[D]_0 = n[DNA] \tag{1b}$$

$$[D] = [D]_0 - [LD] \tag{1c}$$

The titration curves were fit to eq 1a with use of $n$ and the association constant $K_a$ as free parameters, by a commercial data analysis program (Kaleidagraph).

Fluorescence lifetime measurements were conducted with use of an acousto-optic light modulated fluorometer described elsewhere (Piston et al., 1989). The 514-nm line from a Spectra Physics 2035 argon–neon laser was used to excite the 7AACTD samples, with the modulation frequency ranging from 400 kHz to 117 MHz. Data were accumulated relative to a rhodamine B/ethanol solution of similar luminosity, and liftimes and relative amplitudes were obtained from a nonlinear least-squares fit to the phase and modulation data with use of two exponential decays.

*Gel Electrophoresis.* The oligonucleotides in Figure 1 were run on polyacrylamide gels under native conditions in the presence of ACTD. The gel composition was 16% acrylamide (5% cross-linking) in TBM.[1] TBM was also used as the running buffer. ACTD was incorporated into both gels and buffer to a concentration of 1 $\mu$M. The D1, D5, and PL7 oligonucleotides were end labeled with $^{32}$P to a specific activity

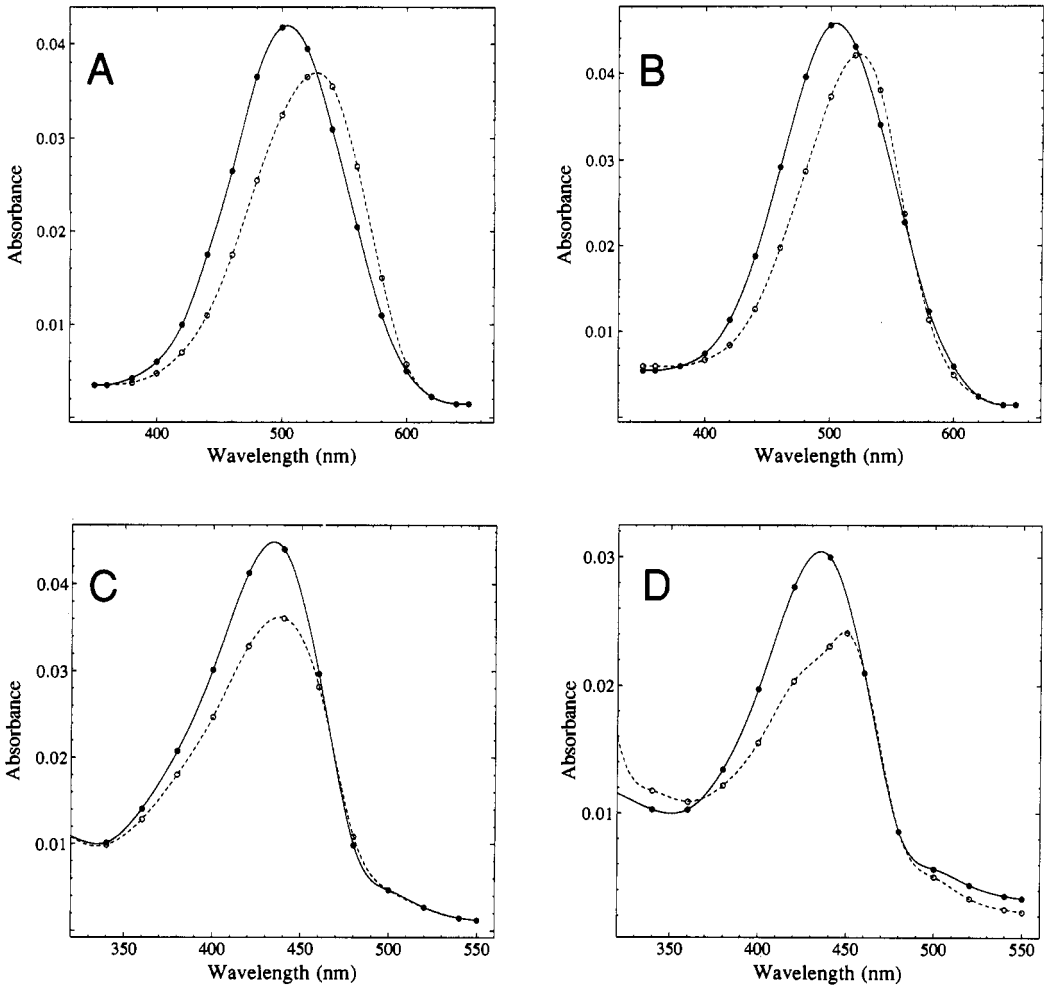


FIGURE 2: Absorption changes for the binding of 7AACTD and ACTD to the oligonucleotides D5 and PL7. The absorption spectrum of the free dye is indicated by the solid lines, and that of the DNA–drug complex is shown by the broken lines. Effects due to dilution are less than 2% of the signal change. (A) 7AACTD (2 $\mu$M) free and in the presence of 3.1 $\mu$M D5 strands. (B) 7AACTD free (2.1 $\mu$M) and in the presence of 6.6 $\mu$M PL7 strands. (C) ACTD free (1.7 $\mu$M) and in the presence of 2 $\mu$M D5 strands. (D) ACTD free (1.2 $\mu$M) and in the presence of 6.6 $\mu$M PL7 strands.

of $10^5$ cpm nmol$^{-1}$ with T4 polynucleotide kinase (New England Biolabs). Samples were electrophoresed at 100 V in a refrigerated room at 7 °C.

Nonradiolabeled samples of D5 and D1 were mixed with an excess of 7AACTD and ACTD and electrophoresed on a 12% acrylamide, TBM-buffered gel in a refrigerated room at 7 °C. The comigration was confirmed by exciting the gel after electrophoresis with an Omega Hyline 546.1-nm Hg line filter and examining the emission from the gel with a Balzers band-pass filter centered at 610 nm with a 50-nm half-width. The fluorescence of the two lanes containing the 7AACTD before ethidium bromide staining and that of the entire gel following addition of the ethidium bromide (excitation by a 302-nm transilluminator table) were recorded using a Photometrics (Tucson, AZ) Series 200 CCD camera. Image processing on a Macintosh IIfx computer was performed with TCL-Image (Delft Center for Image Processing) and NIH Image. The final images were photographed from the computer screen.

## Results and Discussion

*UV Absorption Spectra.* The absorption spectra of ACTD and 7AACTD alone and in the presence of single-stranded DNA are shown in Figure 2. Both PL7 and D5 induced significant hypochromic and bathochromic shifts in the absorption spectra of the two drugs, similar to that observed for the binding of ACTD (Mueller & Crothers, 1968) and 7AACTD (Gill et al., 1975) to double-stranded DNA. With ACTD, there is an isosbestic point at 458 nm for both oligonucleotides. These significant spectral changes are indicative of stacking interactions between the phenoxazone ring system of the drug and the bases of the DNA (Auer et al., 1978), the exact nature of which are not entirely resolved at the present time. Due to the requirement of guanine for the single-strand mode of binding (see below), stacking probably occurs between the drug and the guanine residue of the oligonucleotides, as has been previously observed in crystallographic and solution studies of ACTD and 7AACTD in the presence of d(G), d(C-G), and d(G-C) (Jain & Sobell, 1972; Chiao et al., 1979; Takusagawa et al., 1982).

Thermally resolved absorption spectra of the D5 and PL7 oligonucleotides in the presence and absence of 1:1 concentrations of ACTD (drugs:strand) are shown in Figure 3, and in Figure 4 the absorbance change is plotted as a fraction of the total absorbance difference between 3 and 84 °C. In the absence of drug, the slight hyperchromicity can be entirely attributed to unstacking of the bases in the single strands. We see no evidence for secondary structures in these oligonucleotides over the temperature range examined. Hairpins and bimolecular complexes exhibit pronounced and highly cooperative melting curve transitions (Jovin et al., 1990). Such is not the case with the oligonucleotides used here, and in

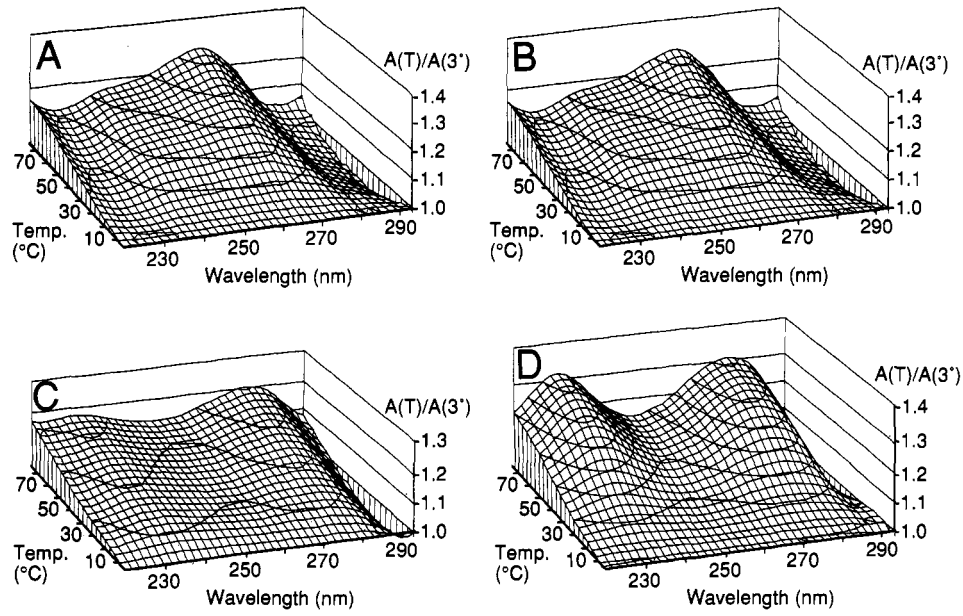


FIGURE 3: Thermally resolved ultraviolet absorption spectra of single-stranded DNAs in the presence and absence of ACTD. Hyperchromicity is expressed as the absorbance ratio $A_\lambda(T)/A_\lambda(3)$; 3 °C is the initial temperature. All spectra were taken in 10 mM sodium cacodylate, pH 7.1/2 mM $MgCl_2$. (A) The D5 oligonucleotide (1.2 μM strands). (B) The D5 oligonucleotide (1.2 μM strands) in the presence of 1.2 μM ACTD. (C) The oligonucleotide PL7 (3.3 μM strands). (D) The oligonucleotide PL7 in the presence of 3.3 μM ACTD.

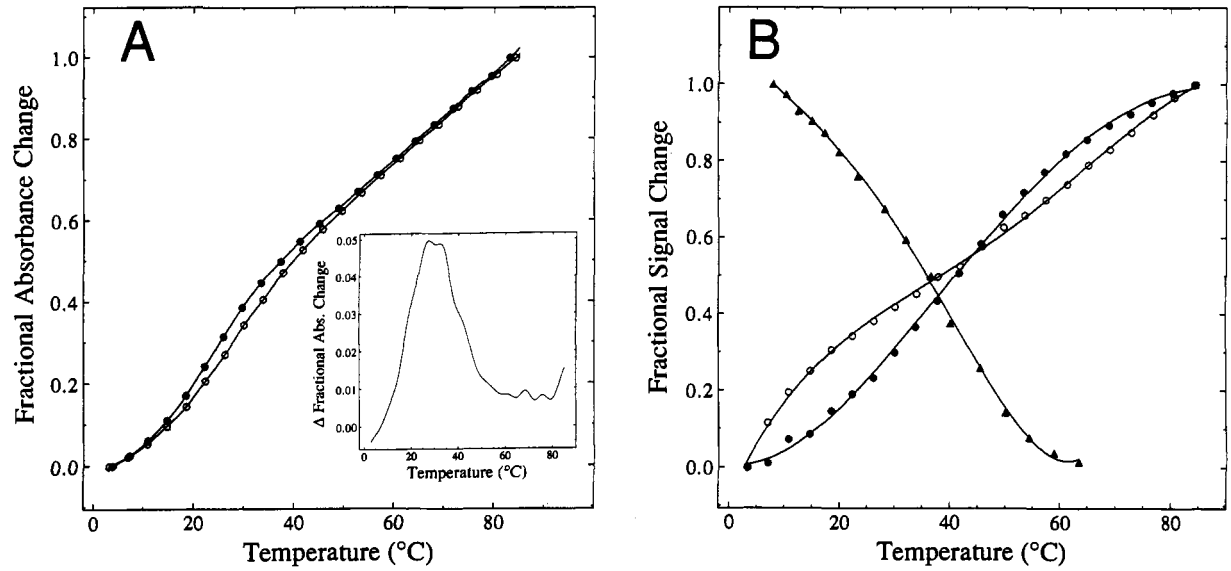


FIGURE 4: Absorbance changes of D5 and PL7 in the presence and absence of ACTD. (A) Fractional absorbance change at 260 nm for D5 in the absence (○) and presence (●) of ACTD, obtained from the melting surfaces shown in Figure 3A,B. The difference in the fractional absorbance change is plotted in the inset and indicates a melting of the D5–ACTD complex at 30 °C. (B) Fractional absorbance change at 264 nm for PL7 in the absence (○) and presence (●) of ACTD, obtained from the melting surfaces shown in Figure 3C,D. The filled triangles indicate the change in fluorescence signal from the 7AACTD–PL7 complex at similar concentrations. The nearly identical $T_m$ (~40 °C) suggests that the complexes between PL7 and both drugs are structurally and thermodynamically similar.

particular, the single-stranded nature of D5 has been extensively demonstrated in other studies (Rippe et al., 1990).

In the presence of 1:1 ratios of ACTD and DNA (strand), little or no change was observed in the D5 thermally resolved profile, indicating that this DNA remained single-stranded even when ACTD was bound. We attribute the changes observed in the thermally resolved profile of PL7 in the presence of ACTD ("hills" at 230 and 280 nm in Figure 3D) to the displacement of the drug from the DNA. The absorption maximum for PL7 is 264 nm and is located in the "valley" of the thermal profile in Figure 3D. The DNA dominates the absorbance at this wavelength, resulting in little or no change in absorption in this region during heating, and indicating that PL7 also remained in the single-stranded form when ACTD was bound. The transition recorded at 264 nm in the PL7–ACTD mixture is plotted in Figure 4B and is compared with that obtained from melting experiments on a PL7–7AACTD mixture monitored by fluorescence. The similar transition temperatures for both drugs indicate that the hyperchromicity observed at 264 nm could be accounted for by the displacement of the ACTD from the oligonucleotide. Thermally resolved curves for complexes of ACTD and DNA duplexes typically exhibit a biphasic melting behavior corresponding to the differential stabilities of the naked and drug-bound DNA (Chen, 1988a; Snyder et al., 1989). Such transitions were not observed with the PL7–ACTD complex.

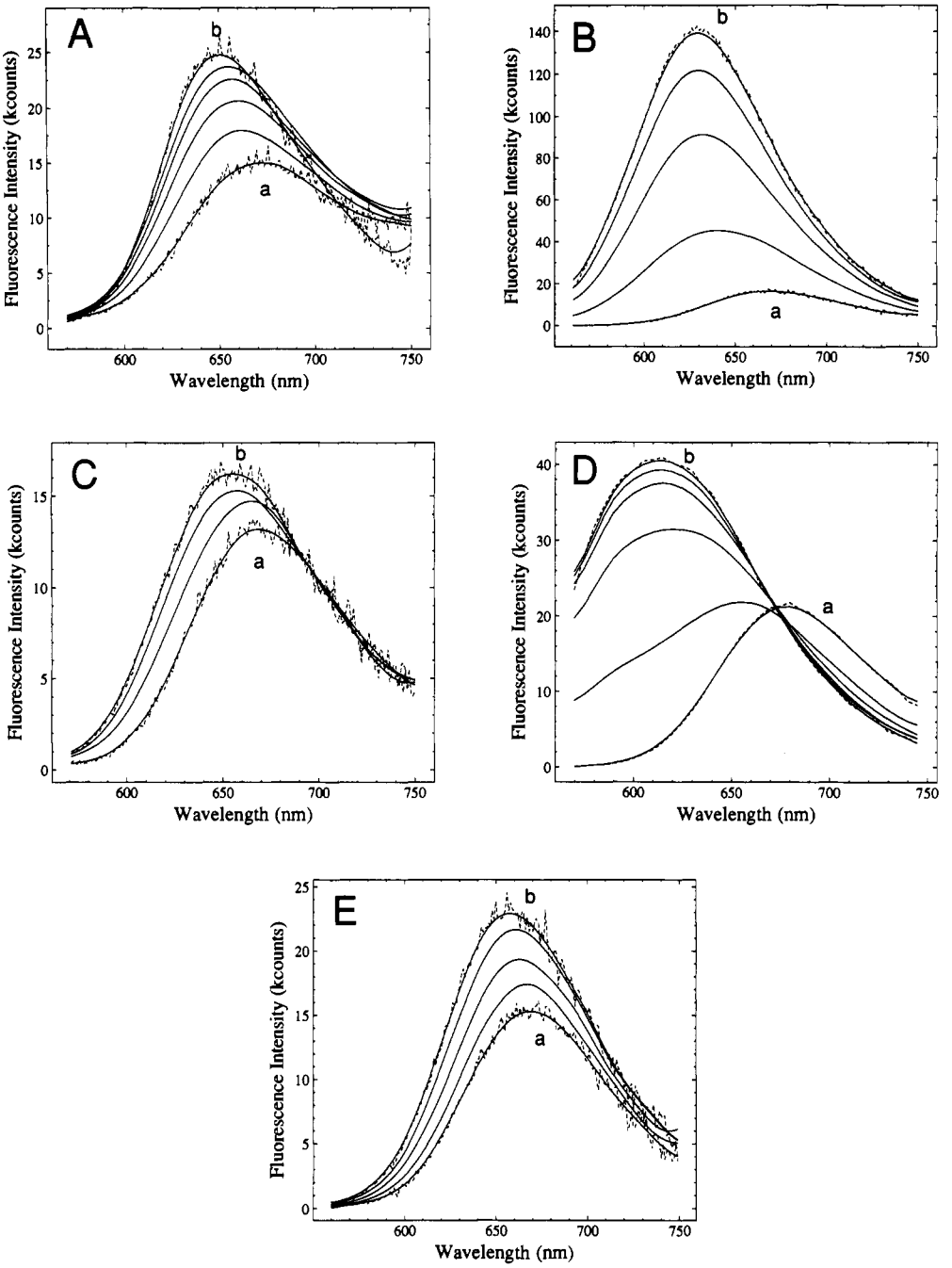


FIGURE 5: Fluorescence spectra of 7AACTD in the presence of DNA. (A) 7 $\mu$M free drug alone (a) and in the presence of 2:1, 3:1, 5:1, 7:1, and 16:1 (b) calf thymus DNA base pairs to drug ratios. (B) 2.5 $\mu$M free drug alone (a) and in the presence of 1:3, 1:2, 1:1.5, and 1:1 (b) D5 strands to drug ratios. (C) 2 $\mu$M free drug alone (a) and in the presence of 1:4, 1:2, and 1:1 (b) D5·D7 duplexes to drug ratios. (D) 24 $\mu$M free drug alone (a) and in the presence of 1:3, 1:1.4, 1:1, 1.5:1, and 2:1 (b) PL7 strands to drug ratios. (E) 2 $\mu$M free drug alone (a) and in the presence of 12:1, 49:1, 98:1, and 170:1 (b) poly(dI) nucleotides to drug ratios. All spectra were taken in 10 mM sodium cacodylate, pH 7.1/2 mM $MgCl_2$. The excitation wavelengths for each DNA–drug solution are those listed in Table I. Actual data for curves a and b are also shown as broken lines, while the solid lines indicate smoothed data from Fourier filtering using the commercial software package Passage.

Analysis according to Ramsing et al. (1989) of the ACTD signal induced by temperature changes at 230 nm (Figure 3D) resulted in a calculated $T_m$ for the PL7–ACTD complex of 40.9 °C, in good agreement with the corresponding 7AACTD fluorescence data (Figure 4B), suggesting that the complexes formed between PL7 and either 7AACTD or ACTD were structurally similar.

*Fluorescence Spectra.* 7-Aminoactinomycin D exhibited a large fluorescence change upon binding to the single-stranded D5 oligonucleotide. The spectra are illustrated in Figure 5B and are compared with those from the drug bound to calf thymus DNA (Figure 5A) and to the D5·D7 antiparallel duplex (Figure 5C). The fluorescent enhancements of the drug bound to the DNA compared to the drug free in solution were calculated by extrapolating plots of inverse fluorescent enhancement vs inverse DNA concentration at the emission maximum of the bound species. The values computed by this method along with the maximum observed signals are listed in Table I. There was a striking difference in the fluorescence enhancement obtained with the single-stranded D5 (~37-fold at 630 nm) and calf thymus DNA (2.9-fold at 650 nm). The latter value is in good agreement with that of 2.5-fold determined in previous studies of 7AACTD bound to calf thymus DNA (Chiao et al., 1979). The fluorescence increase observed

Table I: Physical Characterization of 7-Aminoactinomycin D Binding to Nucleic Acids at 15 °C

| DNA | $\lambda_{em}$[a] | P/D[b] | $F/F_{0\,obs}$ | $F/F_{0\,calc}$[c] |
|---|---|---|---|---|
| 7AACTD, free drug | 670 | | | |
| calf thymus DNA | 650 | 16 | 2.3 | 2.9 |
| D5·D7 | 650 | 66 | 2.0 | 4.2 |
| D5 | 630 | 58 | 27.1 | 36.7 |
| D6 | 670 | 37 | 1.0 | 1.0 |
| D1 | 670 | 66 | 1.0 | 1.0 |
| F9 | 670 | 22 | 1.0 | 1.0 |
| PL7 | 610 | 69 | 18.0 | 22.8 |
| dApdG | 670 | 74 | 1.0 | 1.0 |
| poly(dG) | 670 | 37 | 1.0 | 1.0 |
| poly(dI) | 650 | 206 | 2.4 | 4.0 |

[a] Emission maximum in nanometers with excitation maximum of 540 nm. [b] DNA phosphate to drug ratio at maximum observed fluorescence enhancement. [c] Maximum fluorescence enhancement at the emission peak calculated from the $y$ intercept of an inverse DNA concentration vs inverse change in fluorescence plot.

upon binding of 7AACTD to the D5·D7 duplex was much lower than with D5 alone, and was comparable to that with calf thymus DNA, suggesting that 7AACTD binds even in the absence of a G–C step, as in the case of ACTD complexes with poly[d(TG)]·poly[d(CA)] and poly[d(TC)]·poly[d(GA)] (Wells & Larson, 1970).

In addition to the dramatic fluorescence enhancement of 7AACTD induced by D5, the emission spectrum exhibited a hypsochromic shift from 670 nm for the free dye to 630 nm for the complex. Such a large effect has not been previously reported for any double-stranded DNA (Gill et al., 1975; Chiao et al., 1979). Fluorescence spectra were recorded for 7AACTD in the presence of a variety of single- and double-stranded DNA (Table I and Figure 5). Clearly, not all single-stranded DNAs lead to significant or detectable changes in the fluorescence spectrum of the drug. For example, the single-stranded D6 sequence, which is the same length as D5, induced no spectral change in 7AACTD. Likewise, no spectral change was observed for the D1 sequence, identical with that of the D5 nucleotide except that the guanine residues are replaced by adenine.

To test whether the structural requirement for binding of the drug was satisfied by the presence of an isolated guanine in a sequence, the oligo F9 was mixed with 7AACTD. There was no detectable change in the fluorescence spectrum of the drug (Table I). The same result was obtained with poly(dG) and the dinucleotide dApdG, in good agreement with previous studies of ACTD binding to these DNAs. Poly(dG) does not bind ACTD to any significant extent (Gellert et al., 1965; Wells & Larson, 1970); in the case of dApdG, the association constant is only $1.57 \times 10^3$ $M^{-1}$ (Krugh, 1972). Thus, little binding would have been expected at the concentrations used in our measurements ($\sim 1$ $\mu M$).

Wells and Larson (1970) have shown that ACTD binds to single-stranded poly(dI) with an association constant of $1.3 \times 10^6$ $M^{-1}$, resulting in a slight hypochromicity in the visible absorption spectrum of the drug. The effect of poly(dI) on the fluorescence spectrum of 7AACTD is shown in Figure 5E. Both an enhancement and a blue shift in the fluorescence maximum were observed. However, the change in the fluorescence maximum (−20 nm) was much less than that observed with D5 (−40 nm). The enhancement of 4.0 was similar to that found for calf thymus DNA, but the concentration of poly(dI) required was much higher (Table I).

The effects of the short DNA fragment PL7 on the fluorescence of 7AACTD was investigated (Figure 5D). Both an increase in fluorescence intensity and a blue shift in the emission maximum to 620 nm resulted. However, the emission spectrum was also extremely broad, suggesting that more than one species of bound drug was present. This heterogeneity may reflect the fact that the sequence of the PL7 oligonucleotide has three guanines in nonequivalent locations. Attempts to resolve the emission spectrum by varying the excitation wavelength were unsuccessful, indicating that the ground states of the drug at the various sites were similar, but that the excited states were nonequivalent, presumably due to environmental influences.

Table II: Fluorescent Lifetimes for 7-Aminoactinomycin D and DNA Complexes at 25 °C[a]

| DNA | $\tau$ (ns) | $f$[b] |
|---|---|---|
| buffer | 0.4 | 0.89 |
| | 1.9 | 0.11 |
| D5 | 0.6 | 0.48 |
| | 2.0 | 0.52 |
| PL7 | 0.3 | 0.75 |
| | 1.4 | 0.25 |
| calf thymus DNA | 0.6 | 0.88 |
| | 3.1 | 0.12 |

[a] In 2 mM $MgCl_2$, 10 mM sodium cacodylate buffer, pH 7.1. [b] Steady-state signal fraction = $\alpha_i\tau_i/\sum\alpha_i\tau_i$ where $\alpha_i$ and $\tau_i$ are the amplitudes and lifetimes of the $i$th component.

It is obvious that changes in the 7AACTD emission spectrum, characterized by both fluorescence enhancement and shift of the emission maximum, are good indicators of the binding of 7AACTD to a DNA. Conversely, the lack of spectral change with poly(dG) and dApdG suggests little or no binding. Thus, we have been able to identify three possible outcomes of the interaction of 7AACTD/ACTD with single-stranded DNA: (i) no binding, (ii) binding accompanied by moderate spectral changes, and (iii) binding accompanied by significant spectral changes.

Fluorescence excitation spectra for 7AACTD in the presence of calf thymus DNA, D5, and PL7 were obtained. Only a single excitation band was observed in each case. For calf thymus DNA, the excitation maximum shifted from the free drug maximum of 505 nm to 550 nm for the bound drug. In the presence of D5, the excitation maximum was 540 nm, and with PL7 the excitation maximum was 520 nm. In all cases, the excitation maximum corresponded to the absorption maximum of the bound drug (Figure 2).

*Fluorescence Lifetimes.* The lifetimes of the fluorescence processes of 7AACTD in 10 mM sodium cacodylate buffer (2 mM $MgCl_2$, pH 7.1) are reported in Table II. The free drug was characterized by two distinct lifetimes of 1.9 and 0.4 ns. The shorter component comprised 89% of the measured steady-state fluorescence, a result consistent with the high degree of fluorescence anisotropy observed with the free drug (see below). In the presence of saturating amounts of D5 or PL7, the same two lifetimes were present, but in different ratios. With PL7, the composition of the longer lived component increased to about 25% of the steady-state signal, in agreement with the increase in quantum yield shown in Figure 5D. In the 7AACTD–D5 complex, the longer lived component constituted over 50% of the steady-state signal, corresponding to the large fluorescent enhancement shown in Figure 5B.

The lifetimes for the drug–calf thymus DNA complex were measurably different from those of the drug–single-stranded DNA complexes. Whereas two lifetimes were still present in the calf thymus DNA complex, the lifetime of the second component was noticeably longer (3.1 ns) than that of 1.4–2.0 ns for the free drug or the drug–D5 and drug–PL7 complex. This discrepancy suggests that the mechanism for fluorescent enhancement observed with the single-stranded DNAs is quite different from that involved in 7AACTD–double-stranded

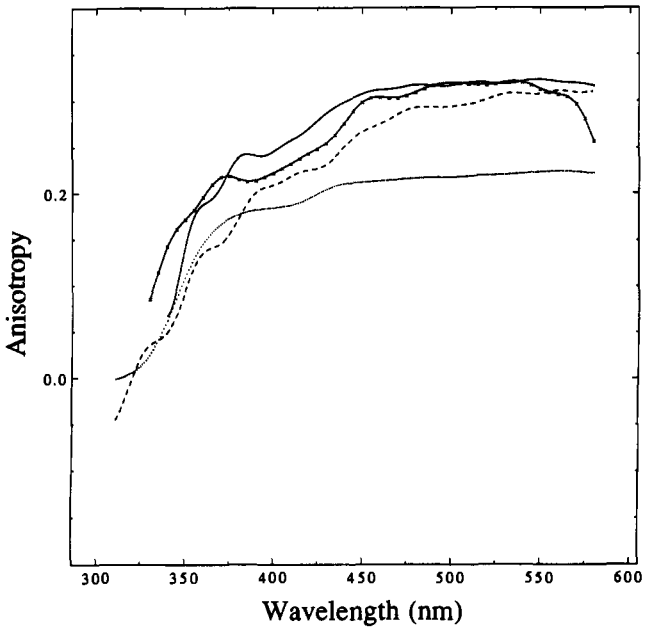


FIGURE 6: Steady-state fluorescence anisotropy of 7AACTD in the absence and presence of DNA. The emission was monitored at the maxima for the DNA used, as listed in Table I, and is corrected for the optics of the instrument. The anisotropy of a 2 $\mu$M solution of free dye is shown (···) along with similar solutions in the presence of 10:1 calf thymus DNA base pairs (- - -), PL7 (-×-) and D5 (—).

DNA interactions. A plausible explanation of the lifetime data would be an equilibrium in solution of two conformational states of the 7AACTD, one possessing a short (0.3–0.6 ns) lifetime and the other possessing a longer (2 ns) lifetime. Binding to the single-stranded DNAs would result in a shift in the equilibrium of the drug conformation favoring the species with the 2-ns lifetime. This component would also contribute more to the observed steady-state fluorescence.

*Fluorescence Polarization Spectra.* The fluorescence anisotropy of the free 7AACTD and the drug bound to calf thymus DNA, D5, and PL7 is plotted in Figure 6. The free drug possesses a considerable anisotropy at 15 °C, due both to its large size and short excited-state lifetime. Complexation with calf thymus DNA led to an increase in the anisotropy (and quantum yield) of fluorescence, indicative of a relatively rigid complex (rotationally restricted) between the DNA and the drug. Complexation of 7AACTD with D5 and PL7 also led to an increase in the anisotropy larger than that obtained with calf thymus DNA and the extreme increase in quantum yield documented above (Figure 5B,D). The relationship among fluorescence anisotropy, fluorescence lifetime, and rotational correlation time of a fluorophore is given by

$$(r_0/r) = 1 + (\tau/\phi) \qquad (2)$$

where $r_0$ is the anisotropy of the completely immobilized fluorophore, $r$ is the measured anisotropy, $\tau$ is the fluorescence lifetime, and $\phi$ is the rotational correlation time. From this relationship, it is clear that any increase in the anisotropy of fluorescence must reflect a decrease in the value for $\tau/\phi$. As shown above, the fluorescence lifetimes for the bound 7AACTD increased relative to the free drug upon binding to calf thymus DNA, D5, and PL7, although not to the same degree (Table II). The fluorescence anisotropy was also greater than that of the free drug (Figure 6). These results indicate that the complexes between the drug and calf thymus DNA, PL7, or D5 were rotationally rigid, leading to longer rotational correlation times. The greater anisotropy and increased (mean) fluorescent lifetime of 7AACTD complexed to D5 and PL7 compared to calf thymus DNA suggest that the rotational correlation times for the former complexes were larger than that for calf thymus DNA. However, without direct determinations of the $\phi$ values or evaluation of possible resonance energy transfer between bound dye molecules, a specific molecular model to explain the observed differences cannot be established. In any event, the greater anisotropy and the increase in the longer lived fluorescent component exclude the possibility of a drug–single-stranded DNA complex in which the drug is loosely bound to the phosphates or in an unstructured association with the bases, since in these two situations the drug would retain considerable rotational mobility in the excited state.

*Titration Curves.* The changes in fluorescence intensity of 7AACTD upon addition of DNA were used to generate binding curves. Figure 7A shows the titration of a solution of 7AACTD with D5 and PL7 at 25 °C. The solid lines are fits obtained using eq 1a. The values of $K_a$ obtained from this data analysis are $4.0 \times 10^6$ $M^{-1}$ ($n = 0.83$) for D5 and $1.1 \times 10^7$ $M^{-1}$ ($n = 0.82$) for PL7. These values indicate that 7AACTD binds much more tightly to the single strands used here than to double-stranded calf thymus DNA, for which $K_a$ is in the range $4 \times 10^4$ to $1 \times 10^6$ $M^{-1}$ (Winkle & Krugh, 1981; Graves & Wadkins, 1989).

The inverse titration of D5 with 7AACTD is also shown in the form of a Scatchard plot in Figure 7B. This analysis led to a binding constant of $2 \times 10^6$ $M^{-1}$ and a saturation value of 0.7 drugs/strand, in good agreement with the titration curve in Figure 7A. Analysis of the original data from Figure 7B using the nonlinearized form of eq 1a (by a nonlinear curve fitting routine) yielded a $K_a$ of $9.1 \times 10^5$ $M^{-1}$ and an $n$ value of 0.71.

*Gel Electrophoresis.* Polyacrylamide gel electrophoresis was carried out with the DNAs shown in Figure 1 under native conditions and at 7 °C in the presence of 1 $\mu$M ACTD (Figure 8). Gels run at 25 °C gave the same result. The electrophoretic mobilities were similar to those obtained in the absence of ACTD (Rippe et al., 1990) and confirm the single-stranded nature of the D5 and PL7 oligonucleotides.

The results of mixing samples of D5 and D1 with 7AACTD and ACTD are shown in Figure 9. The mobilities of all DNAs were identical, indicating that they remained single-stranded in the presence of the drugs. The 7AACTD could be tracked visually as well as by fluorescence as it moved into the gel with the D5 sample. The identical process was also observed with PL7 (data not shown). With D1, the drug remained in the sample well and did not enter the gel. This can be seen, along with the excess drug in lane 1, as the slightly darkened area at the top of lanes 1 and 6 in Figure 9. The fluorescent enhancement observed upon binding of the drug to D5 (Figure 5B) permitted the direct visualization of the bound species. Ethidium bromide staining resulted in the appearance of only one band for each DNA in the gel, and the positions of the bands were identical in the presence and absence of ACTD or 7AACTD. These results indicate that the DNAs remained single-stranded in the presence of bound drug and showed no ordered duplex structures having different gel migration patterns (Rippe et al., 1990; Rippe & Jovin, 1989). We conclude that secondary hairpin or other double-helical structures were not responsible for the observed drug binding.

## Concluding Remarks

The evidence presented here demonstrates that the potent RNA inhibitor actinomycin D (ACTD) and its fluorescent analogue, 7-aminoactinomycin D (7AACTD), bind to sin-

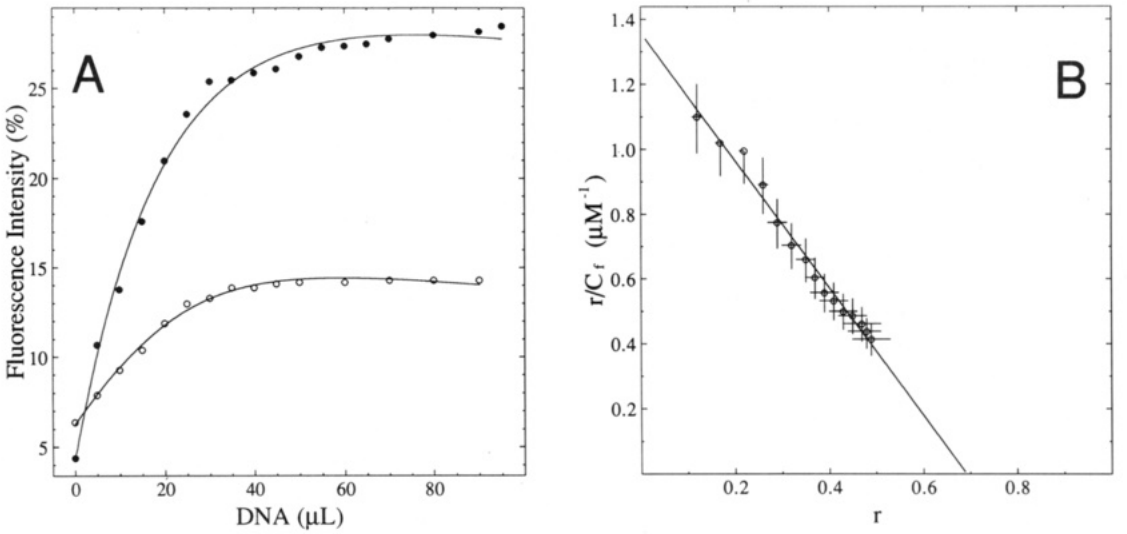


FIGURE 7: Titration curves of 7AACTD with D5 and PL7 oligonucleotides. (A) Titration of 1.1 mL of 0.4 $\mu$M 7AACTD with 8 $\mu$M D5 strands (●) and 1.1 mL of a 0.6 $\mu$M 7AACTD with 7 $\mu$M PL7 strands (○). The solid lines represent best fits to eq 1 from the commercial data analysis program Kaleidagraph. The curves were fit for $n$ (the number of sites per strand) and $K_a$, using the iterative nonlinear least-squares method until the difference in successive iterations was <0.01%. The calculated affinity constants obtained from these curves are $4.0 \times 10^6$ $M^{-1}$ for D5 ($n = 0.83$) and $1.1 \times 10^7$ $M^{-1}$ for PL7 ($n = 0.82$). Fluorescence measurements were obtained by use of a sensitive fluorescence instrument constructed in this laboratory (Loontiens et al., 1991). The intensity is expressed as a percentage of a 0.1-mV full-scale signal produced by the photomultiplier tube of the instrument. (B) A titration of D5 with 7AACTD is shown in the form of a Scatchard plot, with $r$ values in terms of fraction of strands with bound drug. The resulting $K_a$ values is $2.0 \times 10^6$ $M^{-1}$, with an $n$ of 0.7 site/strand (correlation coefficient 0.992). The error bars shown reflect the error from fluctuations in the measured fluorescence signal (±0.1% of 0.1 mV) and indicate the minimum error associated with the Scatchard plot.

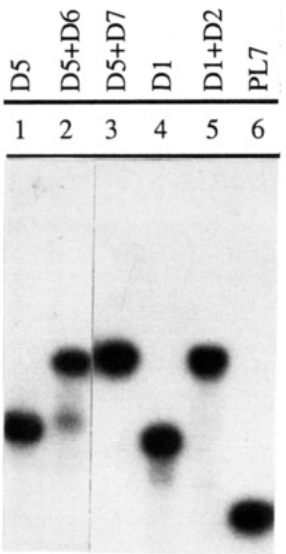


FIGURE 8: Autoradiograph of DNA electrophoresed in the presence of 1 $\mu$M ACTD. Lanes contained 1 $\mu$L of $10^5$ cpm labeled DNA: lane 1, single-stranded D5; lane 2, parallel-stranded D5·D6 duplex; lane 3, antiparallel D5·D7 duplex; lane 4, single-stranded D1; lane 5, single-stranded PL7. No change was observed from samples run in the absence of actinomycin D.

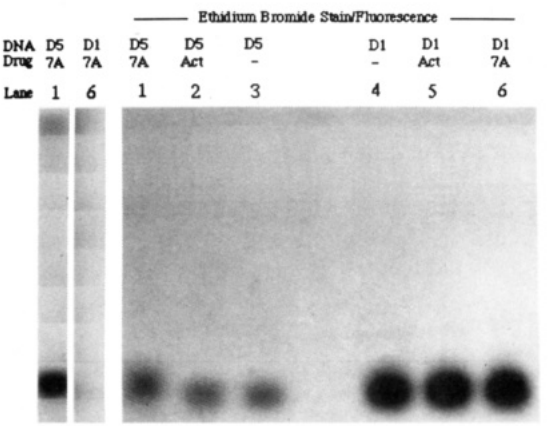


FIGURE 9: Digitized fluorescence image of D5 and D1 oligonucleotides after electrophoresis. Lanes contained 2 $\mu$L of 0.16 mM DNA (strands). Lane 1, D5 + 7AACTD (1:1) (7A); lane 2, D5 + ACTD (1:1) (Act); lane 3, D5 alone; lane 4, D1 alone; lane 5, D1 + ACTD (1:1) (Act); lane 6, D1 and 7AACTD (1:1) (7A). The fluorescence of lanes 1 and 6, containing 7AACTD (7A), is shown before staining with ethidium bromide under excitation with 540-nm light and viewed through a 610-nm-cutoff filter. Unbound drug remained in the wells and can be seen at the top of lanes 1 and 6. The ethidium staining reveals all of the DNA.

gle-stranded DNA. As indicated in Table I, this process has a characteristic requirement for guanine. However, the lack of binding to the F9 oligonucleotide and poly(dG) indicates that not every guanine constitutes a potential binding site, suggesting that ACTD binding to single strands is at least as sequence-specific as in the case of double-stranded DNA.

The changes observed in the fluorescence emission spectrum also argue against a typical double-stranded DNA–7AACTD duplex. Neither the shift in the emission maximum nor the extent of fluorescence enhancement was observed with any double-stranded DNA in our studies or has been reported in previous work (Gill et al., 1975; Chiao et al., 1979), suggesting the existence of a previously undetected drug–DNA complex.

Some of the single-strand DNA–drug complexes are characterized by binding constants larger than those oberved with calf thymus DNA under the same conditions, although the relative influence of cooperative interactions remains to be established. It is interesting to compare the sequences of the D5 and F9 oligonucleotides. If we assume that the guanine residues are required for binding, then the sequence containing three of the four guanines in D5 is $^{5'}$AGT$^{3'}$, whereas in F9 (which binds 7AACTD poorly if at all) it is $^{5'}$TGA$^{3'}$. This finding can be related to the work of Wells and Larson (1970), who reported binding of ACTD to double-stranded poly[d-(GTA)]·poly[d(TAC)] but not to poly[d(GAT)]·poly[d-(ATC)]. In the former, the sequence containing the guanine residue is $^{5'}$AGT$^{3'}$ while in the latter it is $^{5'}$TGA$^{3'}$. Snyder et

al. (1989) reported an unusually high affinity ($K_a$ of $1.4 \times 10^7$ at 37 °C) and nonclassical binding mode for ACTD to the duplex d(CGTCGACG)$_2$, which shares a six-base sequence homology with PL7. In recent work by Chen (1990), enhanced binding of ACTD to oligonucleotide duplexes was observed in the course of thermal denaturation of the DNA. These findings suggest that binding of ACTD to double-stranded DNA may be accompanied, at least in part, by an interaction of a locally perturbed structure with single-stranded characteristics. Such an interaction might partially explain the complex association and dissociation kinetics observed for the binding of ACTD to simple repeating sequences such as [d(GC)]$_n$ (Fox & Waring, 1984; Brown & Shafer, 1987; Chen, 1988a).

The exact sequence(s) required for binding of ACTD is not known at this point. Both D5 and PL7 contain several guanine residues. However, the binding stoichiometries (Figure 7) indicate that only one drug is bound per strand of DNA, suggesting that either only one guanine-containing site in D5 and PL7 is capable of binding ACTD, or the drug excludes all other sites upon binding. This uncertainty cannot be resolved from the binding curves, but the broad emission signal from the PL7 complex argues for the latter situation with this DNA. We have synthesized further D-series oligonucleotides containing single guanine residues, and investigations are currently underway to determine the sequence hierarchy required for single-strand binding by ACTD and 7AACTD.

The possible biological roles of single-strand binding by ACTD and 7AACTD are of some interest. Bunte et al. (1980) have shown that ACTD inhibits hybridization of RNA–DNA duplexes, probably by binding to the single-stranded DNA. This mechanism is proposed to be responsible for the inhibition of DNA elongation by viral RNA-directed DNA polymerase (reverse transcriptase). The same study also indicated that ACTD bound to single-stranded DNAs hindered DNA–DNA duplex formation. Wells and Larson (1970) observed that whereas micromolar amounts of ACTD can inhibit transcription of poly(dI), much higher concentrations are required for the inhibition of poly(dG) transcription, in agreement with the observed ACTD binding ability. ACTD is effective in blocking elongation of RNA from the initiated RNA polymerase–DNA complex, but only if the drug is present from the outset (Straney & Crothers, 1987). It is possible that binding of ACTD to single-stranded DNA located in the open complex may occur and contribute to some extent to the inhibition of elongation. Exactly such a binding mechanism has been postulated by Sobell (1985) for ACTD, in which the drug is bound to $\beta$-DNA (the partially melted region between single-stranded and double-stranded DNA) in the transcriptional complex. Our studies with single-stranded DNAs are compatible with this model. It should be noted that in several footprinting studies (Aivashahvilli & Beabeahashvilli, 1983; Phillips & Crothers, 1986; White & Phillips, 1989a,b) ACTD was found to block RNA elongation predominantly at $^5$GpC$^3$ sites. Blockage of elongation at these sites, coupled with destabilization of the initiated complex in the presence of ACTD, implies that more than one mode of DNA binding by ACTD is responsible for the drug's potent biological activity. Thus, it may be that both the single-stranded binding to DNA observed here and the classical double-stranded DNA intercalation mode are involved in the termination of transcription by ACTD.

## Acknowledgments

We are indebted to Karsten Rippe and Gudrun Heim for help in the DNA synthesis and labeling experiments, to Dr. Robert Clegg for the nonlinear curve fitting routines, and to Dr. Frank Loontiens for many helpful discussions and suggestions.

**Registry No.** ACTD, 50-76-0; 7AACTD, 7240-37-1; D1, 135798-88-8; D2, 135798-90-2; D5, 135798-89-9; D6, 135798-87-7; D7, 135798-86-6; F9, 135798-85-5; PL7, 135760-56-4; dApdG, 4336-87-2; poly(dG), 25656-92-2; poly(dI), 27732-54-3.

## References

Aivasashvilli, V. A., & Beabealashvilli, R. Sh. (1983) *FEBS Lett. 160*, 124–128.
Auer, H. E., Pawlowski-Konopnicki, B. E., Chiao, Y.-C. C., & Krugh, T. R. (1978) *Biopolymers 17*, 1891–1911.
Bittman, R., & Blau, L. (1975) *Biochemistry 14*, 2138–2145.
Bollum, F. J. (1967) in *Procedures in Nucleic Acid Research* (Canton, G. L., & Davies, D. R., Eds.) pp 577–583, Harper & Row, New York.
Brown, S. C., & Shafer, R. H. (1987) *Biochemistry 26*, 277–282.
Bunte, T., Novak, U., Friedrich, R., & Moelling, K. (1980) *Biochim. Biophys. Acta 610*, 241–247.
Chen, F. M. (1988a) *Biochemistry 27*, 1843–1848.
Chen, F. M. (1988b) *Biochemistry 27*, 6393–6397.
Chen, F. M. (1990) *Biochemistry 29*, 7684–7690.
Chiao, Y.-C. C., Rao, K. G., Hook, J. W., Krugh, T. R., & Sengupta, S. K. (1979) *Biopolymers 18*, 1749–1762.
Farber, S. J. (1966) *J. Am. Med. Assoc. 198*, 826–836.
Fox, K. R., & Waring, M. J. (1984) *Eur. J. Biochem. 145*, 579–586.
Gellert, M., Smith, C. E., Nevrille, D., & Felsenfeld, G. (1965) *J. Mol. Biol. 11*, 445–457.
Gill, J. E., Jotz, M. M., Young, S. G., Modest, E. J., & Sengupta, S. K. (1975) *J. Histochem. Cytochem. 23*, 793–799.
Goldberg, I. H., & Friedman, P. A. (1971) *Annu. Rev. Biochem. 40*, 775–810.
Graves, D. E., & Wadkins, R. M. (1989) *J. Biol. Chem. 264*, 7262–7266.
Jain, S. C., & Sobell, H. M. (1972) *J. Mol. Biol. 68*, 1–20.
Jovin, T. M., Rippe, K., Ramsing, N. B., Klement, R., Elhorst, W., & Vojtiskova, M. (1990) in *Structure & Methods, Volume 3: DNA & RNA* (Sarma, R. H., & Sarma, M. H., Eds.) pp 155–174, Adenine Press, Albany, NY.
Kersten, H., & Kersten, W. (1974) in *Inhibitors of Nucleic Acid Synthesis*, pp 40–66, Springer, Berlin.
Krugh, T. R. (1972) *Proc. Natl. Acad. Sci. U.S.A. 69*, 1911–1914.
Lewis, J. L. (1972) *Cancer 30*, 1517–1521.
Loontiens, F. G., McLaughlin, L. W., Diekmann, S., & Clegg, R. M. (1991) *Biochemistry 30*, 182–189.
Mueller, W., & Crothers, D. M. (1968) *J. Mol. Biol. 35*, 251–290.
Phillips, D. R., & Crothers, D. M. (1986) *Biochemistry 25*, 7355–7362.
Piston, D. W., Marriot, G., Radivoyevich, T., Clegg, R. M., Jovin, T. M., & Gratton, E. (1989) *Rev. Sci. Instrum. 60*, 2596–2600.
Ramsing, N. B., & Jovin, T. M. (1988) *Nucleic Acids Res. 16*, 6659–6676.
Ramsing, N. B., Rippe, K., & Jovin, T. M. (1989) *Biochemistry 28*, 9528–9535.
Reich, E. (1964) *Science 143*, 684–689.
Rippe, K., & Jovin, T. M. (1989) *Biochemistry 28*, 9542–9549.
Rippe, K., Ramsing, N. B., & Jovin, T. M. (1989) *Biochemistry 28*, 9536–9541.

Rippe, K., Ramsing, N. B., Klement, R., & Jovin, T. M. (1990) *J. Biomol. Struct. Dyn. 7*, 1199–1209.
Sengupta, S. K., Tinter, S. K., Lazarus, H., Brown, B. L., & Modest, E. J. (1975) *J. Med. Chem. 18*, 1175–1180.
Sentenac, A., Simon, E. J., & Fromageot, P. (1968) *Biochim. Biophys. Acta 161*, 299–308.
Synder, J. G., Hartman, N. G., D'Estantoit, B. L., Kennard, O., Remeta, D. P., & Breslauer, K. J. (1989) *Proc. Natl. Acad. Sci. U.S.A. 86*, 3968–3972.
Sobell, H. M. (1985) *Proc. Natl. Acad. Sci. U.S.A. 82*, 5328–5331.
Straney, D. C., & Crothers, D. M. (1987) *Biochemistry 26*, 1987–1995.
Takusagawa, F., Dabrow, M., Neidle, S., & Berman, H. M. (1982) *Nature 296*, 466–469.
Waring, M. J. (1981) *Annu. Rev. Biochem. 50*, 159–192.
Wells, R. D., & Larson, J. E. (1970) *J. Mol. Biol. 49*, 319–342.
White, R. J., & Phillips, D. R. (1988) *Biochemistry 27*, 9122–9132.
White, R. J., & Phillips, D. R. (1989a) *Biochemistry 28*, 4277–4283.
White, R. J., & Phillips, D. R. (1989b) *Biochemistry 28*, 6259–6269.
Wilson, W. D., Jones, R. L., Zon, G., Scott, E. V., Banville, D. L., & Marzille, L. G. (1986) *J. Am. Chem. Soc. 108*, 7113–7114.
Winkle, S. A., & Krugh, T. R. (1981) *Nucleic Acids Res. 9*, 3175–3186.
Zhou, N., James, T. L., & Shafer, R. H. (1989) *Biochemistry 28*, 5231–5239.

# Cytoplasmic Phosphorylating Domain of the Mannitol-Specific Transport Protein of the Phosphoenolpyruvate-Dependent Phosphotransferase System in *Escherichia coli*: Overexpression, Purification, and Functional Complementation with the Mannitol Binding Domain†

Rob P. van Weeghel, Gert Meyer, Hendri H. Pas, Wolfgang Keck, and George T. Robillard*
*BIOSON Research Institute, University of Groningen, Nijenborgh 16, 9747 AG Groningen, The Netherlands*
*Received February 8, 1991; Revised Manuscript Received June 10, 1991*

ABSTRACT: The cytoplasmic C-terminal domain, residues 348–637, and the membrane-bound N-terminal domain, residues 1–347, of $EII^{mtl}$ have been subcloned and expressed in *Escherichia coli*. The N-terminal domain, $IIC^{mtl}$, contains the mannitol binding site, and the C-terminal domain, $IIBA^{mtl}$, contains the activity-linked phosphorylation sites, His-554 and Cys-384. Overexpression of the BA domain was achieved by a translational in-frame fusion of the gene with the *cro* ATG start codon, downstream of the strong $P_R$ promoter of phage λ. The domain has been purified and characterized in in vitro complementation assays. It possessed no mannitol phosphorylation activity itself but was able to restore the phosphoenolpyruvate-dependent phosphorylation activity of two $EII^{mtl}$ phosphorylation site mutants, lacking His-554 or Cys-384. The complementary N-terminal domain was also expressed. Membranes possessing $IIC^{mtl}$ were unable to phosphorylate mannitol at the expense of phosphoenolpyruvate. However, when the membranes were combined with the purified C-terminal domain, mannitol phosphorylation activity was restored. Mannitol transport and phosphorylation were also restored in vivo when the two plasmids encoding the N- and C-terminal domains were expressed in the same cell. These data demonstrate the existence of structurally and functionally distinct domains in $EII^{mtl}$: a cytoplasmic domain with phosphorylating activity and a membrane-bound N-terminal domain which, in the presence of the cytoplasmic domain, is able to actively transport and phosphorylate mannitol. The ability to separate, overproduce, and purify structurally stable, enzymatically active domains opens the way for 3D structural studies as well as complete kinetic analysis of the activities of the individual domains and their interactions.

Mannitol transport in *Escherichia coli* occurs by the series of reactions shown in Scheme I [for reviews, see Postma and Lengeler (1985) and Robillard and Lolkema (1988)]. Mannitol-specific enzyme II ($EII^{mtl}$)[1] has been extensively purified, and its gene, *mtlA*, has been cloned and sequenced (Jacobson et al., 1979; Lee & Saier, 1983). It consists of a membrane-bound N-terminal domain, which binds mannitol (Grisafi et al., 1989; Lolkema et al., 1991), and a phosphorylating C-terminal domain, located in the cytoplasm. The

Scheme I

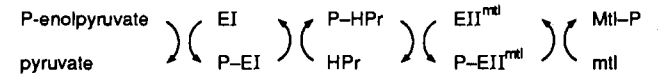


C-terminal domain contains two activity-linked amino acid residues, His-554 and Cys-384, which are transiently phos-

†This research was supported by the Netherlands Foundation for Chemical Research (SON) with financial aid from the Netherlands Organization for the Advancement of Scientific Research.
* To whom correspondence should be addressed.

[1] Abbreviations: PTS, phosphoenolpyruvate-dependent sugar phosphotransferase system; PEP, phosphoenolpyruvate; DTT, dithiothreitol; $EII^{mtl}$, mannitol-specific enzyme II; $EII^{nag}$, *N*-acetylglucosamine-specific enzyme II; $EII^{bgl}$, β-glucoside-specific enzyme II; $IIA^{mtl}$, cytoplasmic domain, residues 490–637; $IIB^{mtl}$, cytoplasmic domain, residues 348–489; $IIBA^{mtl}$, cytoplasmic domain, residues 348–637; $IIC^{mtl}$, N-terminal domain, residues 1–347; ISO, inside-out; $IIA^{man}$, P13 domain of $EIII^{man}$; $IIB^{man}$, P20 domain of $EIII^{man}$.

0006-2960/91/0430-9478$02.50/0 